TWIST - A computer model for stellarator optimization

J. Raeder, H. Gorenflo

IPP 2/270 August 1983

MAX-PLANCK-INSTITUT FÜR PLASMAPHYSIK

8046 GARCHING BEI MÜNCHEN

MAX-PLANCK-INSTITUT FÜR PLASMAPHYSIK

GARCHING BEI MÜNCHEN

TWIST - A computer model for stellarator optimization

J. Raeder, H. Gorenflo

IPP 2/270 August 1983

Die nachstehende Arbeit wurde im Rahmen des Vertrages zwischen dem Max-Planck-Institut für Plasmaphysik und der Europäischen Atomgemeinschaft über die Zusammenarbeit auf dem Gebiete der Plasmaphysik durchgeführt.

IPP 2/270

J. Raeder
H. Gorenflo

TWIST - A computer model for stellarator optimization

in English

August 1983

Abstract

TWIST is a simple computer model of reactor-scale stellarator devices. It allows determination of parameter sets which optimize given objective functions and simultaneously take into account any constraints which may be imposed on any of the model variables.

The model is based on equations describing the geometrical arrangement, together with the plasma, blanket, shield, and magnet system.

Typically, constraints are imposed on the ignition margin, first-wall loads, neutron fluence, coil current density, maximum magnetic induction at the coils, coil tensile stress, neutron dose to the magnets, and dpa's and helium concentration in the first-wall material.

The application of TWIST is demonstrated in sample calculations for reactor-scale devices based on magnetic field configurations of the Wendelstein VII-AS type.

1. Introduction

During the systems studies at IPP the layout of large tokamak experiments and reactors was observed to be governed by the performance objectives aimed at and by the characteristics chosen for the design /1/.

Performance objectives, e.g. the minimum ignition margin to be achieved, and design characteristics, e.g. necessary clearances between adjacent coils, can be included as constraints which have to be met in solving the equations modelling the device. That solution which optimizes a prescribed objective function is kept.

This procedure, which has been described in detail in /1, 2/, was adopted with its basic features unaltered to set up a model for stellarator devices. The model described in this report is still a very simple one. This is mainly due to the fact that much fewer systems studies have been conducted for stellarators than for tokamaks. Many of the model equations are therefore simple first approximations. When some insight into the parametric interdependences of stellarator devices has been gained, the model may be improved step by step via refining or adding equations. This is facilitated by the solution method chosen in /1, 2/, where the individual equations are always evaluated in the same order. The addition of an equation calls for considering whether all input necessary for its evaluation is available

at the position chosen for it in the solution sequence. Formulation of equations which calls for iterations should be avoided because the model is intended as the basis for a fast running computer program which is capable of scanning large parameter spaces.

2. Description of the model

2.1 Geometry

The shape of the minor plasma cross-section is determined by the magnetic surfaces formed by the interaction of the vacuum magnetic field with a finite-ß plasma. The plasma shape varies periodically with the toroidal angular coordinate ϕ, having a total of p periods along the major circumference. By using the area A_{pl} of the plasma cross-section, an average minor plasma radius a_p is defined:

$$a_p = (A_{pl}/\pi)^{1/2} . \qquad (1)$$

Because A_{pl} varies with ϕ in a periodic manner, the toroidal average of A_{pl} will be used in eq. (1). The geometrical centre of the plasma cross-section is situated, on the average, at the major radius R_p.

The plasma is surrounded by a chamber with an elliptic minor cross-section (see Fig. 1). Its minor half-axis a_w is chosen to be

$$a_w = a_p + d_{pw} , \tag{2}$$

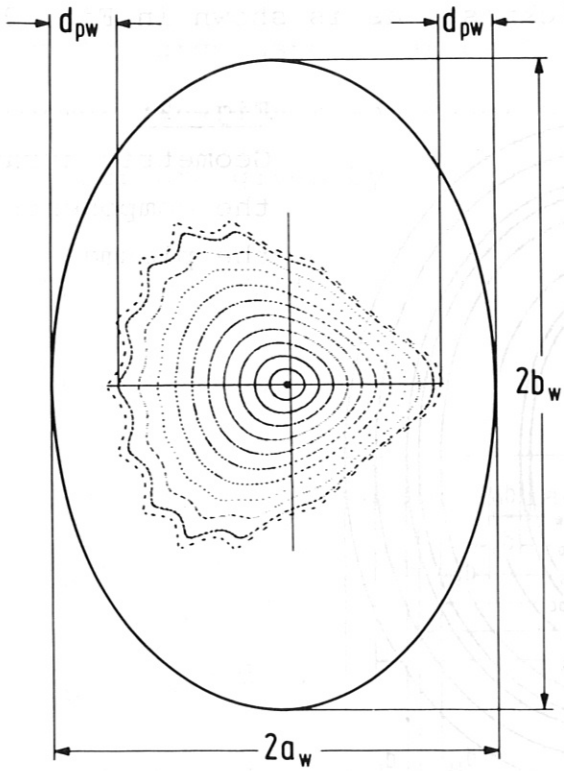

Fig. 1: Geometry of plasma and first-wall surface

d_{pw} being the distance between the inner and outer edges of the plasma and the inner contour of the chamber (see Fig.1). The choice of eq. (2) is based on the assumption that there exist toroidal locations where the plasma cross-section does not strongly deviate from being circular, as is illustrated in Fig. 1. If the plasma cross-section is

everywhere strongly elliptical, a_p in eq. (2) has to be replaced by a length which is about equal to the toroidal average of the minor half-axes of the plasma.

All components surrounding the plasma are modelled as toroidal shells with elliptic minor contours, each with a certain radial thickness, as is shown in Fig. 2.

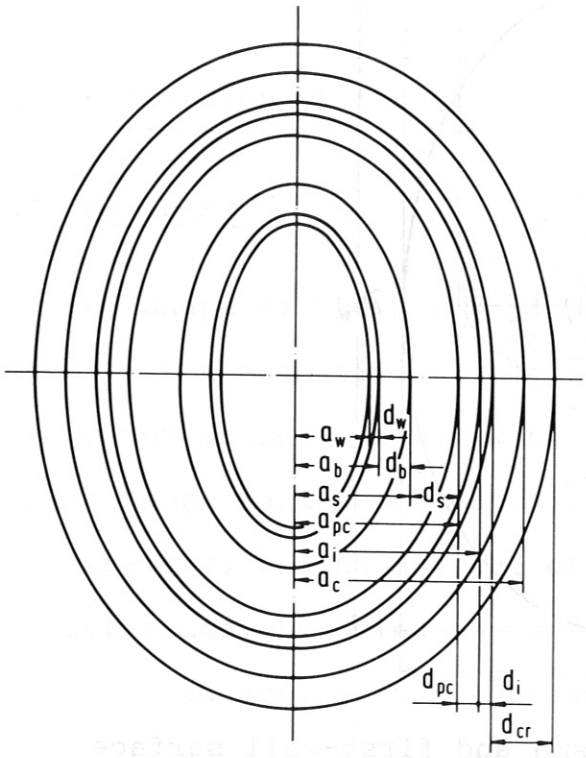

Fig. 2:
Geometric arrangement of the components surrounding the plasma

The inner chamber wall facing the plasma is characterized by the minor half-axis a_w following from eq. (2) and the major half-axis

$$b_w = e_w \cdot a_w \,, \tag{3}$$

e_w being the vertical elongation of the chamber inner wall. The thickness of the chamber wall is d_w.

The blanket thickness d_b is determined from the required T-breeding. It is assumed constant all around the plasma. This simple assumption is made because, for the time being, no problems are anticipated in connection with space requirements in the centre of the device and with magnetic field economy. This is due to stellarator specific features such as the presumably large aspect ratios A_p and the omission of the OH transformer. The minor and major half-axes of the inner blanket contour are given by

$$a_b = a_w + d_w \,, \tag{4}$$

$$b_b = b_w + d_w \,. \tag{5}$$

The blanket is surrounded by a radiation shield with thickness d_s and the half-axes

$$a_s = a_b + d_b \,, \tag{6}$$

$$b_s = b_b + d_b \tag{7}$$

of the inner contour.

Behind the blanket a clearance of thickness d_{pc} is provided which may remain empty but may be necessary for finding a consistent set of device parameters which both optimizes the objective function selected and meets all constraints imposed by physics, technology, design and topology.

The clearance may also be used to accommodate a ring-like structure to support the radial magnetic forces acting on the coils. Such a concept has been proposed in /3/.

The half-axes of the inner edge of the clearance are:

$$a_{pc} = a_s + d_s \,, \tag{8}$$

$$b_{pe} = b_s + d_s \,. \tag{9}$$

The clearance is enclosed by the casing and the thermal insulation of the magnetic field coils, which has a thickness d_i. The half-axes of the inner contour are

$$a_i = a_{pc} + d_{pc} \,, \tag{10}$$

$$b_i = b_{pc} + d_{pc} \,. \tag{11}$$

The coil is characterized by its centre line, which has the half-axes

$$a_c = a_i + d_i + d_{cr}/2 \,, \tag{12}$$

$$b_c = b_i + d_i + d_{cr}/2 \,. \tag{13}$$

The magnetic field is generated by a total of N_c coils. In general, the toroidal modulation of the coil conductors varies from coil to coil within one field period, but is periodically repeated p times (p = number of field periods

along one toroidal revolution. The lateral extension d_{tc} of the coils is given in units of the radial thickness d_{rc}:

$$d_{ct} = \varepsilon_{rt} \, d_{cr} \, . \tag{14}$$

For simplicity, the major axes of all ellipses are assumed to coincide with the major axis of the elliptical coil centre line. In an actual device the orientation of the major axis of the centre line with respect to the main torus axis may oscillate periodically with the toroidal angle ϕ . This modulation may, for example, facilitate generation of a desired flux surface pattern by coils the minor cross-section of which has been made elliptical to simplify manufacture.

2.2 Basic equations

The following equations together with the constraints to be treated later (Sec. 2.3) form the basis of the model.

The equations are written in MKSA units if not otherwise stated.

2.2.1 Geometric relations

A plasma aspect ratio A_p is defined by

$$R_p = A_p \, a_p \, . \tag{15}$$

The various volumes involved - penetrations are not considered here - are given by

$$V_p = 2\pi^2 \, a_p^2 \, R_p \tag{16}$$

(V_p = plasma volume),

$$V_w = 2\pi^2 \, d_w \, (a_w+b_w+d_w) R_p \tag{17}$$

(V_w = first-wall volume),

$$V_b = 2\pi^2 \, d_b \, (a_b+b_b+d_b) R_p \tag{18}$$

(V_b = blanket volume),

$$V_s = 2\pi^2 \, ds \, (a_s+b_s+d_s) R_p \tag{19}$$

(V_s = volume of the shield surrounding the blanket),

$$V_{pc} = 2\pi^2 \, d_{pc} \, (a_{pc}+b_{pc}+d_{pc}) R_p \tag{20}$$

(V_{pc} = volume of the clearance between the outer edge of the radiation shield and the inner edge of the thermal insulation for the coils),

$$V_i = 2\pi^2 \, d_i \, (a_i+b_i+d_i) R_p \tag{21}$$

(V_i = volume of coil casing and thermal insulation protecting the coils).

The volume of a single coil is given by

$$V_c = g_c \cdot \pi d_{cr} d_{ct} (a_c+b_c) . \tag{22}$$

The factor g_c (≥ 1) describes the increase of the coil volume caused by the toroidal modulation of the modular field coils assumed. The size of g_c mainly depends on the amplitude of the toroidal modulation and the l-number of the stellarator field predominantly to be generated by the coils. In general, g_c will vary from coil to coil within one field period so that an average value of g_c has to be used when calculating the total coil volume V_{ct} from

$$V_{ct} = N_c V_c . \tag{23}$$

The total coil volume V_{ct} comprises the volumes of the conductor, stabilizer, reinforcing material,cooling ducts, and electrical insulators.

The area A_w of the inner wall surface is given by

$$A_w = 2\pi R_p \cdot l_w \tag{24}$$

(l_w = circumference of the first-wall contour facing the plasma); l_w is approximated by

$$l_w = \pi (a_w+b_w) [1+(a_w-b_w)^2/4(a_w+b_w)^2] . \tag{25}$$

This formula is accurate within $2 \cdot 10^{-4}$ up to $b_w/a_w = 2$.

2.2.2 Relations pertaining to the plasma

The normalized rotational transform $t = \iota / 2\pi$ (ι = rotational transform angle) at the plasma edge is a strong functional of the coil configuration. The main parameters determining t are the l-number, the coil aspect ratio $A_c = R_p/(a_c\, b_c)^{1/2}$, the toroidal amplitude a_{ct} of modular coils, and the number p of field periods. Therefore t is written as

$$t = t\,(l,\ A_c,\ a_{ct},\ p,\ \ldots). \tag{26}$$

For a system with l = 2 the authors of /5/ propose formulae which lead to

$$t = \Delta\phi_{ct}^2 / (4p\varepsilon_c^4) \tag{27}$$

($\Delta\phi_{ct}$ = toroidal modulation amplitude in angular units, $\varepsilon_c = 1/A_c$); we assume that $\Delta\phi_{ct}$ will be of order $2\pi/N_c$. To allow numerical results to be represented by a formula generalizing eq. (26), the following relation will be used for l = 2:

$$t = g_c \cdot \pi^2/(p^{\alpha p}\, N_c^{\alpha N}\, \varepsilon_c^{\alpha\varepsilon}). \tag{28}$$

The factor g_c, and the exponents αp, αN, $\alpha\varepsilon$ have to be taken from numerically calculated magnetic field distributions.

The maximum average ß-value (useful part of the total ß) achievable is determined from a function to be specified for the actual case treated:

$$\beta = \beta\ (t, A_p, l, \ldots) \tag{29}$$

(ß = volume average, t = rotational transform at the plasma edge in units of 2π). The parameters explicitly displayed in eq. (25) presumably are the basic ones if ß is limited by plasma equilibrium.

For a configuration with l = 2 the relation

$$\beta = g_\beta \cdot t^2/A_p \tag{30}$$

shall be used. The basic scaling $\beta \sim t^2/A_p$ is taken from /4/. The factor g_β has to be taken from numerical calculations of plasma equilibria with finite ß-values.

We characterize the plasma energy balance by a dimensionless parameter, the "ignition margin":

$$c_i = \varepsilon_\alpha \cdot p_\alpha/p_t \tag{31}$$

(p_α = α-heating power density, p_t = transport loss power density for a reference situation, ε_α = fraction of α-power trapped by the plasma. The value $c_i = 1$ describes a system with transport losses according to the reference rate which are just covered by the trapped α-particle heating power. Additional losses such as

bremsstrahlung, impurity line radiation or transport losses which exceed those anticipated by the p_t used in eq. (31) are described by an appropriate enhancement of c_i above unity if an ignited plasma has to be treated. Driven systems are characterized by $c_i < 1$.

In general, p_α/p_t depends on the physical and geometric parameters of the plasma (t, ß, A_p, a, temperatures, profiles). The actual relations between the parameters determining $\varepsilon_\alpha p_\alpha/p_t$ have to be determined by using a numerical transport code.

For a stellarator plasma the slowest transport that can be expected is "neoclassical", possibly with some reduction by tying the particle drift orbits as closely as possible to the magnetic surfaces ("drift optimization").

To get an insight into parametric dependences, we evaluate $\varepsilon_\alpha p_\alpha/p_t$ for neoclassical particle and energy transport in the plateau regime for both electrons and ions. With no radiation losses at all, $T_i \sim T_e$, $p_\alpha \sim \beta^2 B_o^4 \langle\sigma v\rangle/T_i^2$, and $p_{tr} \sim \beta\ T_i^{3/2}/t\ A_p\ a_p^3$, this leads

$$\beta\ t\ A_p\ a_p^3\ B_o^4 \sim c_i T_i^{7/2}/\varepsilon_\alpha \langle\sigma v\rangle \qquad (32)$$

(B_o = magnetic induction at the plasma centre, T_i = volume average of the ion temperature, T_e = volume average of the electron temperature, $\langle\sigma v\rangle$ = fusion reaction parameter).

Because $\langle\sigma v\rangle \sim T_i^2$ is approximately valid in the range $8 \lesssim T_i \lesssim 20$ keV, one gets roughly

$$\beta\, t\, A_p\, a_p^3\, B_o^4 \sim c_i T_i^{3/2}/\varepsilon_\alpha \,. \qquad (33)$$

Hence the value of the parameter combination $\beta\, t\, A_p\, a_p^3\, B_o^4$ for ignition ($c_i = 1$) in a regime dominated by neoclassical transport losses increases rather strongly with T_i.

To determine the variation of $\beta\, t\, A_p\, a_p^3\, B_o^4$ with T_i precisely, a numerical solution of the stationary energy and particle balances for a plasma with DT ions ($m = 2.5$), electrons, and no radiation losses has been used /6/. Figure 3 shows $f_{z\beta} = f_{z\beta}(T_i) = \beta\, t\, A_p\, a_p^3\, B_o^4$ for various cases ($\varepsilon_\alpha = 1$). The solutions used are globally stable against thermal runaway because p_t ($\sim nT^{5/2}$) increases more steeply with T than p_α ($\sim n^2T^2$) if the density n is determined by a fixed refuelling rate.

The two cases treated are characterized by $R_p = 24$ m, $a_p = 1.65$ m ($A_p = 14.55$) together with $t = 0.6$, $B_o = 5.2$ T or $t = 0.4$, $B_o = 5.755$ T. For these two sets of parameters the product $t\, A_p\, a_p^3\, B_o^4$ is the same. Refuelling in both cases is assumed to occur according to the strongly peaked spatial distribution $(\partial n/\partial t)_{ref} \sim [1-(r/a_p)^2]^{10}$. The amplitude of the radial profile is varied. This variation leads to a scan of T_i, T_e and n. The actual value of β is calculated from

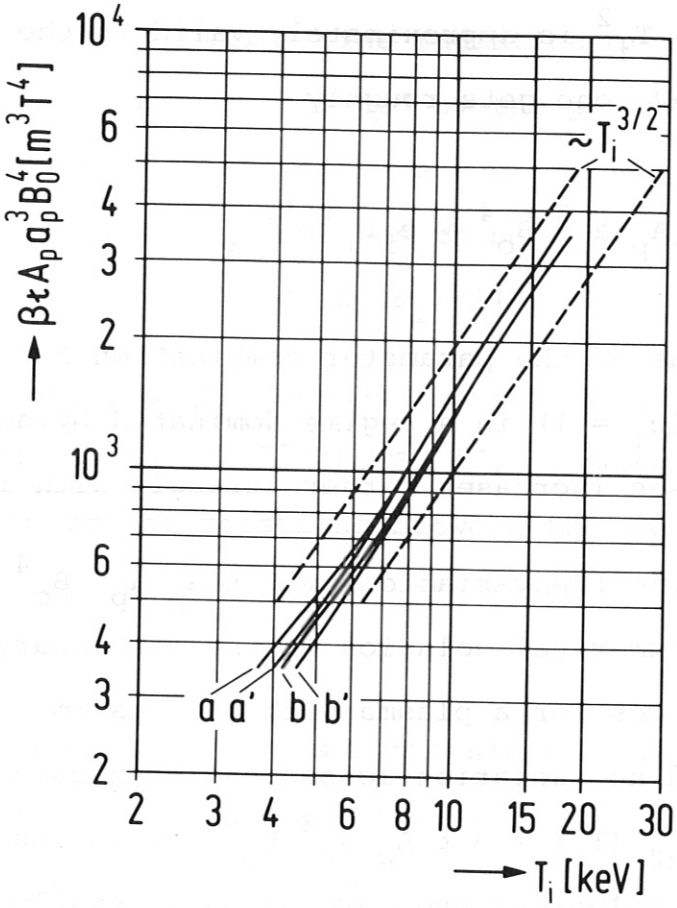

Fig.3: Parameter combination $\beta\, t\, A_p\, a_p^3\, B_o^4$ vs. T_i for $\varepsilon_\alpha = 1$, $c_i = 1$; common parameters: $A_p = 24/1.65 = 14.545$, $a_p = 1.65$ m, refuelling profile $\sim [1-(r/a_p)^2]^{10}$, helical ripple $\varepsilon_h = \varepsilon_o + \varepsilon_1 \cdot (r/a_p)^2$ with $\varepsilon_o = 3$ %, $\varepsilon_1 = 15$%.

curve a : $t = 0.6$, $B_o = 5.2$ T, neoclassical transport

curve b : $t = 0.4$, $B_o = 5.755$ T, neoclassical transport

curve a': $t = 0.6$, $B_o = 5.2$ T, neoclass.+anomalous transport

curve b': $t = 0.4$, $B_o = 5.755$ T, neoclass.+anom.transport

these results. The products of ß with $tA_p\ a_p^3\ B_o^4$ as functions of T_i are displayed in Fig. 3. The two curves for t = 0.4 and 0.6 do not completely coincide. This is due to the transport processes assumed: (1) neoclassical transport for the electrons including the $1/\nu$-contribution (ν = Coulomb collision frequency) due to the helical ripple /6/; (2) neoclassical plateau transport for the ions even in the regime of long mean free paths /7/. A model helical ripple distribution $\varepsilon_h = \varepsilon_o + \varepsilon_1 \cdot (r/a_p)^2$ with ε_o = 3 %, ε_1 = 15 % was used throughout. The $1/\nu$-contribution to the electron transport makes the transport depend on the density and hence causes the slight difference between the curves for t = 0.4 and 0.6.

Because no radiation losses at all have been accounted for and ε_α is equal to unity, all results are characterized by $c_i = 1$.

The relation $\beta\, t\, A_p\ a_p^3\ B_o^4 \sim T_i^{3/2}$ is confirmed by the numerical calculations as being a reasonable approximation (see the dashed lines in Fig. 3).

The addition of an anomalous electron heat conduction according to the evaluation of experimental results presented in /8/ alters the result only slightly (see the small deviations between the $\beta\, t\, A_p\ a_p^3\ B_o^4$-curves for low values of T_i in Fig. 3).

The scaling with respect to A_p and a_p given by eq. (31) was reproduced by using R_p = 20 m instead of 24 m together with a_p = 1.807 m instead of 1.65 m. The corresponding variations are so small that they cannot be discriminated in Fig. 3.

In the optimization program the ignition margin c_i of a plasma with the actual parameters ß, t, A_p, a_p and B_o is calculated from

$$c_i = \varepsilon_\alpha \, ß \, t \, A_p \, a_p^3 \, B_o^4 / f_{zß} \, , \qquad (34)$$

where $f_{zß}$ is the parameter combination $ß \, t \, A_p \, a_p^3 \, B_o^4$ characteristic of an ideal case chosen to normalize the actual combination $\varepsilon_\alpha \, ß \, t \, A_p \, a_p^3 \, B_o^4$ in order to yield the dimensionless parameter c_i defined by eq. (31). As the ideal situation we use that exemplified by the curves a and b in Fig. 3 (neoclassical plateau transport for the ions, complete neoclassical electron transport, complete trapping of α-power by the plasma, i.e. $\varepsilon_\alpha = 1$). Hence $f_{zß}$ is an input paramter which depends on T_i and profile shapes as has been demonstrated above. Typical values for $f_{zß}$ may be taken from Fig. 3 if the operating temperature of the reactor plasma has been chosen and the profiles are similar to those shown in Fig. 6.

If transport laws other than the predominantly neoclassical ones of the previous description are used, eq. (34) has to be replaced by an appropriate relation. For ALCATOR scaling

($\tau_E \sim n\, a_p^2$), for example, the appropriate relation would be $c_i = \varepsilon_\alpha\, \beta^2\, a_p^2\, B_o^4/f_{z\beta}$, where $f_{z\beta}$ is approximately proportional to T_i and again depends on the profiles of n and T. The fusion power density (plasma volume average) is calculated from

$$p_f = \gamma_f \cdot \beta^2\, B_o^4 \quad . \tag{35}$$

For the DT reaction the factor γ_f is of the order $2 \cdot 10^{-6}$ (MKSA units; β is a pure number, not in per cent). It depends on both the profile shapes of n and T. Because γ_f is essentially proportional to $\langle\sigma v\rangle/T^2$, it exhibits a flat maximum for T_{ni} between 10 and 20 keV (T_{ni} is the density weighted volume average of the ion temperature). In Fig. 4 various curves γ_f vs. T_{ni} are shown.

Fig. 4: Factor γ_f vs. T_{ni} for various cases.

Square profiles of n and T:

- curve a : $\langle\sigma v\rangle$ from table /10/,
- curve a': $\langle\sigma v\rangle$ from formula /9/.

Profiles of n and T resulting from $c_i = 1$, $A_p = 24/1.65 = 14.545$, $a_p = 1.65$, refuelling profile $\sim [1-(r/a_p)^2]^{10}$, helical ripple $\varepsilon_h = \varepsilon_o + \varepsilon_1 (r/a_p)^2$ with $\varepsilon_o = 3$ %, $\varepsilon_1 = 15$ %:

$\langle\sigma v\rangle$ from formula /9/:

- curve b : $t = 0.6$, $B_o = 5.2$ T neoclassical transport
- curve c : $t = 0.4$, $B_o = 5.755$ T " "
- curve d': $t = 0.6$, $B_o = 5.2$ T neoclass. + anomalous "
- curve e': $t = 0.4$, $B_o = 5.755$ T " + " "

$\langle\sigma v\rangle$ from table /10/:

- curve d : $t = 0.6$, $B_o = 5.2$ T neoclass.+anom.transport
- curve e : $t = 0.4$, $B_o = 5.755$ T " + " "

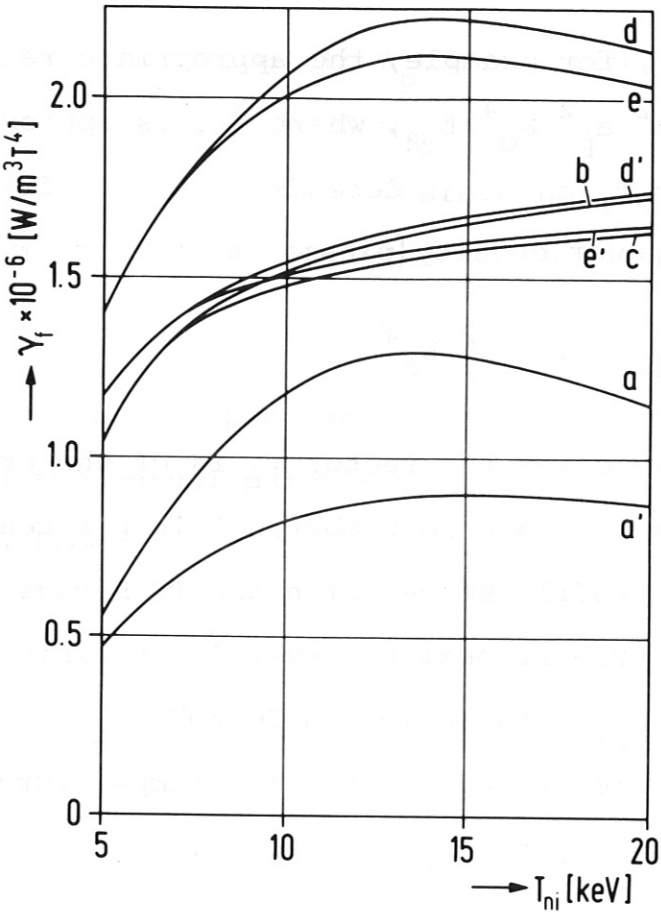

Fig. 4

Curve a' is valid for square profiles of n and T together with $\langle\sigma v\rangle$ according to the well known formula $\langle\sigma v\rangle = 3.68 \times 10^{-18}\ T^{2/3} \cdot \exp(-19.94/T^{1/3})$ $\langle\sigma v\rangle$ in m^3/s, T in keV given in /9/. This formula for $\langle\sigma v\rangle$ has been used in all energy balance calculations cited in this paper - if not otherwise stated - because it was used in the original version of the computer program /6/. In fact, this analytical approximation yields appreciably lower $\langle\sigma v\rangle$-values for 5 keV < T < 30 keV than those contained in the table in /10/, which is in common use. The values of $\langle\sigma v\rangle$ from the above formula and from the tables are shown in Fig.5. The maximum deviation in the range of interest for us occurs between T = 8 keV and T = 15 keV. It amounts to a factor 1.43 at T = 10 keV.

Curve a in Fig. 4 has been calculated for comparison with curve a'. Again square profiles for n and T were used but $\langle\sigma v\rangle$ was taken from the table mentioned. The γ_f-values according to curve a are well above those from curve a'. The maximum exhibited is more pronounced. It occurs at $T_{ni} \simeq 13.5$ keV.

The values of γ_f for a given value of T_{ni} become much higher if the profiles of n and T are no longer square but peaked. This well-known fact rests on the n^2-scaling of the fusion reaction rate and on the strong increase of $\langle\sigma v\rangle$ with T in the interval of interest for a DT fusion plasma.

Fig. 6 shows various calculated profiles of n and T normalized to their central values. The shapes of all T-profiles closely coincide. The same is true of the n-profiles. This is valid although a wide range of central temperatures ($T_i(0) \simeq 4.5$ to 21.5 keV), central densities from 4 to $8 \times 10^{20}\ m^{-3}$, c_i between 1 and 1.2, and the inclusion as well as the exclusion of anomalous transport are covered.

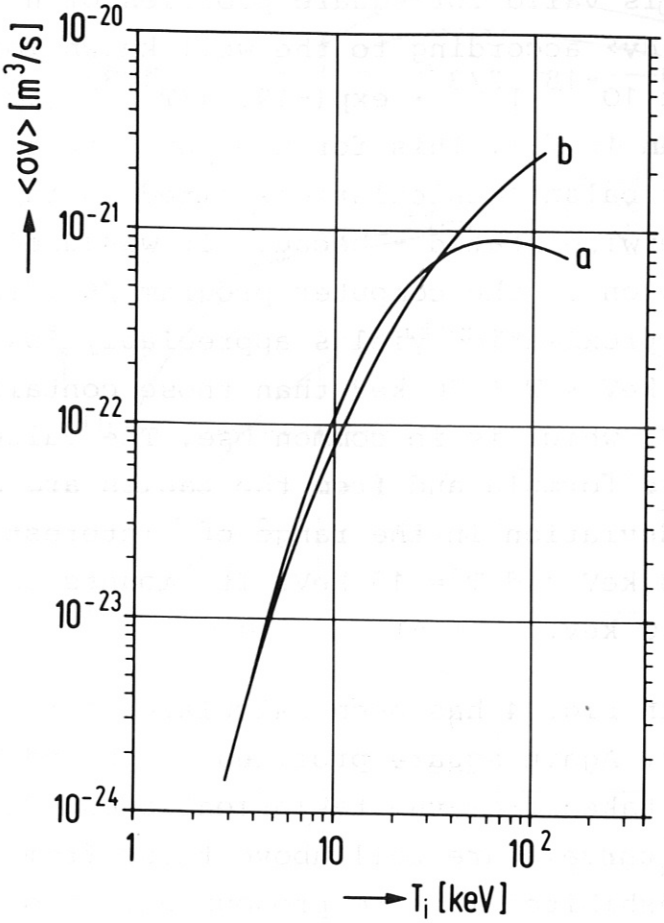

Fig. 5: curve a: <σv> according to the table in /10/;
curve b: <σv> a-cording to the formula in /9/.

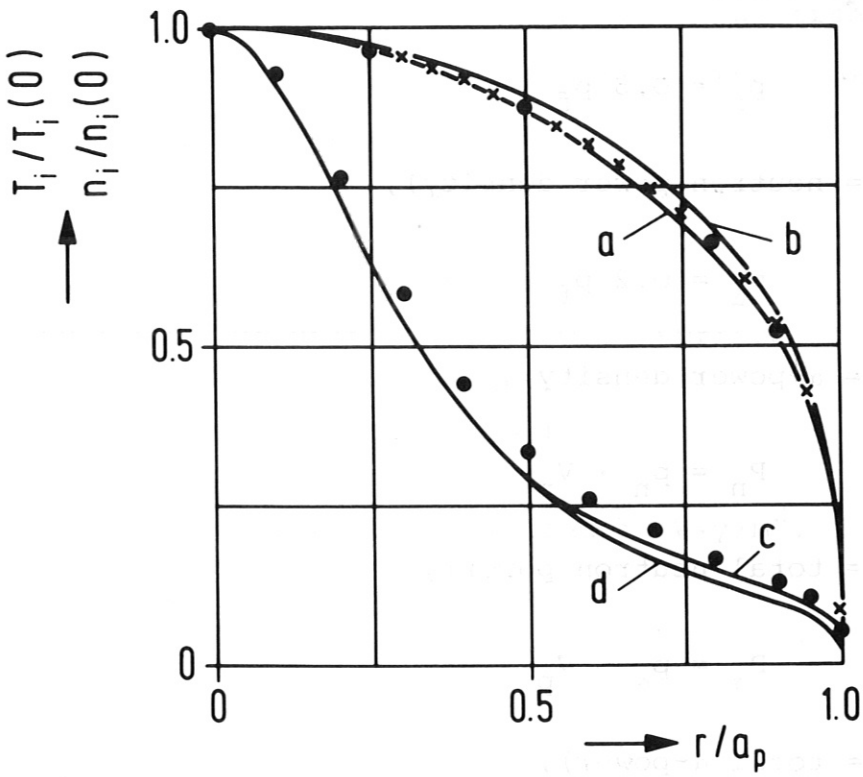

Fig. 6: Radial profiles of n and T corresponding to t = 0.6, B_o = 5.2 T, A_p = 24/1.65 = 14.545, a_p = 1.65 m, refuelling profile $\sim [1-(r/a_p)^2]^{10}$, helical ripple $\varepsilon_h = \varepsilon_o + \varepsilon_1 \cdot (r/a_p)^2$, ε_o = 3 %, ε_1 = 15 %:

- curve a : T-profile, $T_i(0)$ = 6.62 keV, neoclassical transport, c_i = 1
- curve b : T-profile, $T_i(0)$ = 21.69 keV, neoclassical transport, c_i = 1
- curve c : corresponds to curve a: n-profile, $n_i(0) = 4.05 \times 10^{20}\ m^{-3}$
- curve d : corresponds to curve b: n-profile, $n_i(0) = 8.52 \times 10^{20}\ m^{-3}$

x : neoclassical + anomalous transport; T_{ni} = 10 keV, n = $1.35 \times 10^{20}\ m^{-3}$, ß = 4.1 %, c_i = 1.19

⊗ : as in case x but <σv> from the table in /10/; T_{ni}=10 keV; n=$1.15 \times 10^{20} m^{-3}$, ß=3.6%, c_i=1.12.

All quantities related to the fusion power are calculated on the basis of the fusion power density p_f given by eq. (35):

$$p_n = 0.8\ p_f \tag{36}$$

(p_n = neutron power density),

$$p_\alpha = 0.2\ p_f \tag{37}$$

(p_α = α-power density),

$$P_n = p_n \cdot V_p \tag{38}$$

(P_n = total neutron power),

$$P_\alpha = p_\alpha \cdot V_p \tag{39}$$

(P_α = total α-power),

$$P_f = P_n + P_\alpha \tag{40}$$

(P_f = total fusion power),

$$P_{th} = M_{bl} \cdot P_n + P_\alpha \tag{41}$$

(P_{th} = total thermal power, M_{bl} = factor of energy multiplication caused by exothermic nuclear reactions in the blanket),

$$q_n = P_n/A_w \tag{42}$$

(q_n = neutron power per unit of first-wall surface),

$$q_\alpha = P_\alpha / A_w \tag{43}$$

(q_α = α-power per unit of first-wall surface; q_α is not necessarily equal to the heat flux density to be transmitted through the first wall because of divertors or limiters which may be present),

$$q_f = P_f / A_w \tag{44}$$

(q_f = fusion power per unit of first-wall surface),

$$Q_n = q_n \cdot \tau_{tot} / (3.154 \times 10^7) \tag{45}$$

(Q_n = time-integrated neutron wall load in $W \cdot y/m^2$, τ_{tot} = full power burn time in s).

2.2.3 Relations pertaining to the magnet system

The relations compiled in this sections are simple estimates which are only meant to serve as zero-order approximations. They will have to be refined if specifically tailored coil systems are to be included in the optimization procedure.

As a basis the average B_o of the magnetic induction taken along the average plasma cross-section centre line is used. The relations resting on B_o are as follows:

$$H_o = B_o/\mu_o \ , \tag{46}$$

$$I_{ct} = 2\pi R_p \cdot H_o \tag{47}$$

(I_{ct} = total current in the coils surrounding the plasma),

$$I_c = I_{ct}/N_c \tag{48}$$

(I_c = average current per coil, N_c = total number of coils),

$$j_c = I_c/(d_{cr} d_{ct}) \tag{49}$$

(j_c = gross winding current density; the area $d_{cr} \cdot d_{ct}$ comprises conductor, stabilizer, reinforcing material, electric insulators and helium cooling channels),

$$B_{cm} = B_{cm}(B_o, \text{ geometry}). \tag{50}$$

B_{cm} is the maximum magnetic induction which occurs at one or more locations of the coils. Owing to the lack of axisymmetry in stellarator configurations the enhancement of B_{cm} with respect to B_o is greater than that given by

$$B_{cm} = B_o \ R_p/(R_p - a_c + d_{rc}/2). \tag{51}$$

Equation (51) only accounts for toroidicity but neglects the effects produced by toroidal modulations of the coils. These modulations lead to current concentrations and additional curvatures. The corrections to be applied to eq. (51) have to be taken from numerical or analytical calculations once the type of coils has been specified. To our present knowledge B_{cm}/B_o is about 2 for $A_p \simeq 15$ /14/.

The magnetic energy stored in the magnetic field configuration is approximately given by

$$E_m = 2\pi^2 R_p a_c b_c \cdot B_o^2/2\mu_o \; . \tag{52}$$

The maximum tensile stress σ_{cm} is estimated from

$$\sigma_{cm} = g_\sigma E_m \, \rho_c/M_{ct} = g_\sigma \cdot E_m/V_{ct} \tag{53}$$

(ρ_c = average mass density of the coils, M_{ct} = total mass of coil system, V_{ct} = total coil volume). The scaling used in eq. (53) is based on a generalized virial theorem /11/; the factor g_σ has to be taken from coil designs supported by finite-element stress calculations. To our present knowledge g_σ amounts to about 3 /12/.

2.2.4 Relations pertaining to nuclear aspects

Some parameters which will most probably have to meet constraints are determined by nuclear reactions in the first-wall, blanket and shield areas. The formulae given in the following are based on a parametric study of various breeding materials /13/, from which the figures and relations valid for a blanket composed of Li_2O and 316 SS steel have been taken as representative.

The tritium breeding ratio T is given by the following formula, which closely approximates the numerical results:

$$T = f_T \cdot 1.289\ [1-\exp(-d_b/0.144)] \qquad (54)$$

(d_b = blanket thickness in m). The dimensionless figure f_T (≤ 1) takes into account features such as incomplete coverage of the plasma surface by the blanket or voids caused by the cooling lines.

The energy multiplication M_{bl} due to exothermic nuclear reactions in the first wall and blanket is approximated by

$$M_{bl} = f_M \cdot 1.274\ [1-\exp(-(d_w+d_b)/0.1212)] \qquad (55)$$

(d_w = first wall thickness in m, d_b = blanket thickness in m). The factor f_M corresponds to f_T introduced by eq. (54).

The neutron dose ds_{nc} affecting the coils behind their shielding is given by

$$ds_{nc} = 4.44\text{x}10^{11} \cdot f_c\ q_n \tau_{tot} \cdot \exp(-d_b/0.12) \cdot \exp(-d_s/0.0776) \qquad (56)$$

(ds_{nc} in neutrons/m^2, q_n in W/m^2, τ_{tot} in s, d_b and d_s in m). The first exponential factor in eq. (56) describes the neutron flux attenuation by the blanket, the second the action of the radiation shield. The factor f_c is the ratio of collided to uncollided neutron flux density at the blanket front edge.

The total number of displacements per atom (dpa) of the first wall material is given by

$$d_{pa} = 11.6 \times 10^{-6} \cdot q_n \tau_{tot} / (3.154 \times 10^7) \qquad (57)$$

(q_n in W/m^2, τ_{tot} in s).

The concentration of He atoms produced in the first-wall material by (n,α)-reactions is given by

$$n_{He} = 174 \times 10^{-6} \cdot q_n \tau_{tot} / (3.154 \times 10^7) \qquad (58)$$

(n_{He} in ppm, q_n in W/m^2, τ_{tot} in s).

2.3 Constraints

Some of the quantities determined from the set of model equations may have to meet constraints imposed by technological limitations, design characteristics, and performance objectives.

The constraints which can be imposed in the present version of the model are as follows:

$$N_c \, d_{ct} \leq 2\pi (R_p - a_c - 0.5 \, d_{cr}) \qquad (59)$$

(the sum of the toroidal coil thicknesses must not exceed the available space at the main axis side of the torus),

$$c_i \geq c_{i,min}, \tag{60}$$

$$P_{th,min} \leq P_{th} \quad P_{th,max}, \tag{61}$$

$$q_n \leq q_{n,max}, \tag{62}$$

$$q_\alpha \leq q_{,max}, \tag{63}$$

$$Q_{n,min} \leq Q_n \leq Q_{n,max}, \tag{64}$$

$$j_c \leq j_{c,max}, \tag{65}$$

$$B_{cm} \leq B_{cm,max}, \tag{66}$$

$$\sigma_{cm} \leq \sigma_{cm,max}, \tag{67}$$

$$T \geq T_{min}, \tag{68}$$

$$ds_{nc} \leq ds_{nc,max}, \tag{69}$$

$$dpa \leq dpa_{max}, \tag{70}$$

$$n_{He} \leq n_{He,max}. \tag{71}$$

2.4 Optimization

The aim of the optimization is to find a set of numerical values for a set of fundamental variables. We chose the following set:

t = rotational transform/2π, see eq. (28);

R_p = plasma major radius (see beginning of Sec. 2.1);

d_{pc} = clearance between blanket and coils, see Fig. 2;

d_s = shielding thickness, see Fig. 2;

d_{cr} = radial coil thickness, see Fig. 2;

B_o = average magnetic induction at the plasmas' geometrical centre;

N_c = total number of magnetic field coils;

p = number of toroidal field periods.

The model equations together with the constraints do not, in general, uniquely determine the above set of variables. To define the problem completely, an objective function is introduced, which depends on the above variables. That combination of variables which maximizes (or minimizes) the numerical value of the objective function is considered as being the solution of the model equations.

The optimization procedure is exactly as described in /2/. The details will therefore not be repeated here. For each of the variables an interval is given as input. For each point of the parameter space thus spanned the model equations are evaluated and the corresponding constraints are checked. From all combinations of variables meeting the constraints the one optimizing the objective function is retained. In the environment of this solution a refined grid is spanned and the procedure is repeated, until a desired accuracy limit (imposed on the objective function, for example) is met.

The above procedure is performed for fixed values of the integer variables N_c and p. After a solution has been found, the procedure is repeated using other discrete values out of the intervals specified for N_c and p. Those values of N_c and p which optimize the objective function together with the values for the continuous variables form the final solution.

3. Sample calculations

3.1 Parameters

Equation (28) for t is specified to be

$$t = 1.44 \times \pi^2/(p\, N_c^{\,2}\, \varepsilon_c^{\,4}) \;, \tag{72}$$

which means that

$$g_c = 1.44 \;,$$
$$\alpha p = 1 \;,$$
$$\alpha N = 2 \;,$$
$$\alpha \varepsilon = 4 \;.$$

The value $g_c = 1.44$ stems from magnetic field calculations for W VII-AS type configurations with reactor dimensions /14/. The values for αp, αN, and $\varepsilon\alpha$ are taken from the scaling relations for l = 2 stellarators given in /5/.

For ß we adopt eq. (30) in the form

$$\beta = t^2/A_p \ , \tag{73}$$

which means that

$$g_\beta = 1.$$

The parameter $f_{z\beta}$ in eq. (34) for the ignition margin c_i is chosen to be

$$f_{z\beta} = 6 \times 10^2 \ ,$$

which according to Fig. 3 corresponds to

$$T_i = 6 \text{ keV (volume average of the ion temperature).}$$

To be consistent with T_i = 6 keV and the underlying profiles, we use for the fusion power density in eq. (35)

$$\gamma_f = 1.7 \times 10^6 \text{ W/m}^3 \text{ T}^4 \text{ (see Fig. 4).}$$

For the remaining parameters to be given we use

ε_α	= 0.9	eq. (31), α-trapping efficiency
g_c	= 1.3	eq. (22)
g_σ	= 3 Pa·m^3/J	eq. (53)
e_w	= 1.5	eq. (3), elongation of plasma chamber
ε_{rt}	= 1	eq. (14), coil thickness/width
d_{pw}	= 0.1 m	eq. (2), distance plasma-wall
d_w	= 0.01 m	Fig. 2, wall thickness
d_i	= 0.1 m	Fig. 2, insulation thickness
f_T	= 0.9	eq. (54), blanket coverage for T
f_M	= 0.9	eq. (55), blanket coverage for M_{bl}
T	= 1.1	eq. (54), tritium breeding ratio
τ_{tot}	= 3.154 x 10^{7}s=1a	total burn time.

3.2 Constraints

$c_i \geq 2$,

$1.0\ MW/m^2 \leq q_n \leq 1.5\ MW/m^2$,

$j_c \leq 2.5 \times 10^7\ A/m^2$,

$\sigma_{cm} \leq 2 \times 10^8\ Pa$,

$ds_{nc} \leq 5 \times 10^{21}$ neutrons/m^2 ,

$dpa \leq 100$,

$n_{He} \leq 1.500$.

3.3 Objective function

As objective function we use a highly simplified expression for the direct capital cost of the major torus components plus auxiliary heating:

$$\begin{aligned} DCC = {} & 100\ (DM/kg) \cdot M_W + 100\ (DM/kg) \cdot M_b \\ & + 25\ (DM/kg) \cdot M_s + 100\ (DM/kg) \cdot M_i \\ & + 320\ (DM/kg) \cdot M_{ct} + 0.2/c_i \cdot 5\ (DM/W) \cdot P_\alpha \ . \end{aligned} \quad (74)$$

M_w, M_b, M_s, M_i, M_{ct} are the masses of the first wall, blanket, shield, thermal insulation plus coil casing, and all coils calculated from the respective volumes (see Sec. 2.2.1) and estimated average mass densities. The last term in eq. (74) is the cost of auxiliary heating.

3.4 Results

For lack of a realistic relation between the magnetic induction B_o on axis and the maximum induction B_{cm} at the coils we fix B_o at 5.2 T. This value leads to B_{cm} = 8 to 9 T for W VII-AS type coil configurations of reactor scale.

We keep the values p = 5 and N_c = 50 fixed.

The optimum solution determined by the STOP program set up on the basis of the material presented in Sec. 2 is characterized by:

$t = 0.6904$

$R_p = 17.6884$ m

$d_s = 0.3715$ m

$d_{pc} = 0$

$d_{cr} = 0.6982$ m

DCC = 1.0 (rel. units)

$c_i = 2$, (constraint met)

$q_n = 1.5$ MW/m^2 (upper constraint met)

$Q_n = 1.5$ MWy/m^2

$j_c = 1.8870 \times 10^7$ A/m^2

$\sigma_{cm} = 2 \times 10^8$ Pa (constraint met)

$ds_{nc} = 5 \times 10^{21}$ neutrons/m^2 (constraint met)

dpa = 17.4

$n_{He} = 261$ ppm

a_p = 1.7695 m

A_p = 9.9964

a_w = 1.8695 m

b_w = 2.8042 m

a_c = 3.1264 m

b_c = 4.0611 m

r_c = $(a_c b_c)^{1/2}$ = 3.5632 m

ß = 0.04769

$\mathbf{P}_f$ = 2.8268 MW/m^3

P_f = 3.0903 GW

P_{th} = 3.3753 GW

P_α = 618.06 MW

d_b = 0.4263 m

The optimum combination of numerical values for the variables t, R_p, d_s, d_{pc}, and d_{cr} is within the ranges which were given for these variables.

To exemplify the case of an optimum produced by a variable assuming one of its two prescribed limiting values, we now restrict t to the range $0.t \leq t \leq t_{max}$ with t_{max} between 0.60 and 0.69. This means that t has to be smaller than t_{opt} = 0.6904.

The optimum solution is always reached for a t attaining its maximum admissible value. The constraints on c_i, ds_{nc}, and σ_{cm} ($c_i \geq 2$, $ds_{nc} \leq 5 \times 10^{21}$ neutrons/m², and $\sigma_{cm} \leq 2 \times 10^{8}$ Pa) are again met for all values of t_{max}. The upper limit on q_n ($q_n \leq 1.5$ MW/m²) is no longer

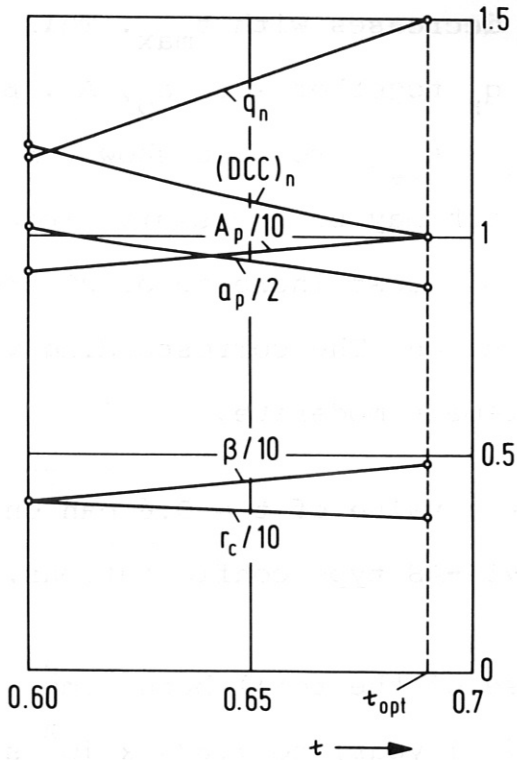

Fig. 7: Some characteristic variables as functions of t (limited to values smaller than t_{opt} = 0.6904); q_n in MW/m^2, a_p in m, r_c im m, ß in %; DCC is normalized to its value for $t = t_{opt}$.

reached but q_n decreases with t_{max}. This is shown in Fig. 7, which displays q_n together with a_p, A_p, ß, r_c, and DCC. The values for $t_{max} = t_{opt}$ are also shown. A limitation of t_{max} to 0.6, which may be necessary, for example, for physical reasons leads to a cost increase of 20 % with respect to the optimum solution. The corresponding variations of a_p, A_p, ß, and r_c remain moderate.

At present a value of t = 0.6 can only be attained at $A_p \simeq 15$ for W VII-AS type configurations.

An increase of the total burn time τ_{tot} from 3.154×10^7 s (= 1 year) to 7.885×10^8 s (= 25 y) but leaving unchanged all parameters characterizing our first example lead to the following optimum sets of values:

$t = 0.7599$

$R_p = 18.5075$ m

$d_s = 0.6216$ m

$d_{pc} = 0.0113$ m

$d_{cr} = 0.7224$ m

DCC = 1.0821 (rel. units)

$c_i = 2$ (constraint met)

$q_n = 1.5$ MW/m^2 (upper constraint met)

$Q_n = 37.5$ MWy/m^2

$j_c = 1.8441 \times 10^7$ A/m^2

$\sigma_{cm} = 2 \times 10^8$ Pa (constraint met)

$ds_{nc} = 5 \times 10^{21}$ neutrons/m^2 (constraint met)

dpa = 435

$n_{He} = 6525$ ppm

a_p = 1.6077 m

A_p = 11.5121

a_w = 1.7077 m

b_w = 2.5615 m

a_c = 3.2380 m

b_c = 4.0918 m

r_c = $(a_c b_c)^{1/2}$ = 3.6399 m

ß = 0.0502

p_f = 3.1281 MW/m^3

P_f = 2.9536 GW

P_{th} = 3.2259 GW

P_α = 590.7 MW

d_b = 0.4264 m.

As expected, a major change is the increase of the shield thickness d_s from 0.3715 m to 0.6216 m. The variations of all other values remain moderate. This is most probably due to the fact that the increase of τ_{tot} is reflected in the highly simplified objective function merely by the increased shield thickness but not via other routes such as maintenance (provision of first-wall replacement, for example) or availability (cost for reliability of auxiliary heating, for example). Both sample calculations should be considered as examples of how to use TWIST. They give some insight into consistent parameter sets of reactor scale stellarators but do not yet form part of a systematic study.

Acknowledgements

The assistence by K. Borrass, E. Harmeyer, F. Rau, M. Söll, and H. Wobig is gratefully acknowledged.

References

/1/ Borrass K., M. Söll: "SUPERCOIL, a layout model for tokamaks with superconducting TF coils", Institut für Plasmaphysik, Report 4/207 (1982)

/2/ Borras K., M. Söll: "Normal conducting steady-state toroidal magnet systems for ignited tokamaks", J. of Fusion Energy, 2, 1 (1982) 71

/3/ Brossmann U., S. Mukherjee: "New supporting concept for large twisted coils", 12th Symp. on Fusion Technology (SOFT), Jülich (1982) D-24

/4/ Solov'ev L.S., V.G. Shafranov: "Plasma confinement in closed magnetic systems" in "Reviews of plasma physics", edited by M.A. Leontovich, Consultants Bureau, New York, London, Vol. 5 (1970) 131

/5/ Hitchon W.N.G., P.C. Johnson, C.J.H. Watson: "Parameter and cost optimizations for a modular stellarator reactor", Culham Laboratory, Report CLM-P 682(1982)

/6/ Wobig H.: private communications

/7/ Wobig H.: "Numerical evaluation of neoclassical transport in stellarators at arbitrary collisionality", Z.Naturforsch. 37a (1982) 906

/8/ Gruber O.: "Scaling of plasma transport in ohmically heated tokamaks", Nucl.Fus. 22, 10 (1982) 1349

/9/ Glasstone S., R.H. Lovberg: "Controlled thermonuclear reactions", Van Nostrand Reinhold Company (1960) 20

/10/ Miley G.H., H. Towner, N. Ivich: "Fusion cross-sections and reactivities", University of Illinois, Report COO-2218-17 (1974)

/11/ Longmire C.L.: "Elementary plasma physics", Interscience Publishers, New York, London (1963) 68

/12/ Harmeyer E: private communication

/13/ Dänner W., H. Gorenflo: "Breeding materials in model blankets: a comparative study", Inst.f.Plasmaphysik, Report 2/268 (1983)

/14/ Rau F.: private communication.